Dynamic Contact Forces on Leukocyte Microvilli and Their Penetration of the Endothelial Glycocalyx

Yihua Zhao,* Shu Chien,* and Sheldon Weinbaum[†]

*Department of Bioengineering and the Whitaker Institute of Biomedical Engineering, University of California, San Diego, La Jolla, California 92093; and [†]Center for Biomedical Engineering and Department of Mechanical Engineering, CUNY Graduate School and City College of New York, New York, New York 10031 USA

ABSTRACT　We develop a theoretical model to examine the combined effect of gravity and microvillus length heterogeneity on tip contact force (F_z^m) during free rolling in vitro, including the initiation of L-, P-, and E-selectin tethers and the threshold behavior at low shear. F_z^m grows nonlinearly with shear. At shear stress of 1 dyn/cm^2, F_z^m is one to two orders of magnitude greater than the 0.1 pN force for gravitational settling without flow. At shear stresses >0.2 dyn/cm^2 only the longest microvilli contact the substrate; hence at the shear threshold (0.4 dyn/cm^2 for L-selectin), only 5% of microvilli can initiate tethering interaction. The characteristic time for tip contact is surprisingly short, typically 0.1–1 ms. This model is then applied in vivo to explore the free-rolling interaction of leukocyte microvilli with endothelial glycocalyx and the necessary conditions for glycocalyx penetration to initiate cell rolling. The model predicts that for arteriolar capillaries even the longest microvilli cannot initiate rolling, except in regions of low shear or flow reversal. In postcapillary venules, where shear stress is ~2 dyn/cm^2, tethering interactions are highly likely, provided that there are some relatively long microvilli. Once tethering is initiated, rolling tends to ensue because F_z^m and contact duration will both increase substantially to facilitate glycocalyx penetration by the shorter microvilli.

INTRODUCTION

Adhesion of circulating leukocytes (or white blood cells, WBC) to vascular endothelial cells (EC) during inflammation and immune surveillance is initiated by the adhesive tethering of the L-, P-, and E-selectins (Lawrence and Springer, 1991; Ley, 1996) and α_4 integrins (Tözeren et al., 1994; Alon et al., 1995b; Berlin et al., 1995) to ligands that are located on either the tips of the WBC microvilli or the EC surface (Berlin et al., 1995; von Andrian et al., 1995). Stein et al. (1999) have shown in vivo that the distribution of adhesion receptors on the WBCs has an important impact on the initiation of tethering, which is confined nearly exclusively to the microvilli tips during free rolling. However, once tethering is initiated, ectodomains on the cell body are equally likely to be involved in adhesive interaction. This result is consistent with Chen and Springer's observation that once tethered rolling is initiated more adhesion sites are recruited to stabilize the rolling velocity as the shear rate is increased (Chen and Springer, 1999). Both studies suggest that tethered rolling involves much larger adhesive contact forces that are sufficient to compress microvilli, applanate the WBC membrane, and thereby create a larger potential for adhesive interaction. The study by Shao et al. (1998) shows that the elastic constant for a microvillus is 43 pN/μm and that a force of 61 pN is

required to pull a single tether. The average characteristic time to achieve the full elastic response is estimated to be 0.77 s.

In contrast to these relatively large tethering and deformation forces, the compressive force acting on a microvillus tip for a WBC resting on a tripod of three microvilli in a gravitational field is of the order of 0.1 pN. The characteristic contact time for a single microvillus in a free-rolling interaction at 1 dyn/cm^2 is of the order of 1 ms and the duration of a single tethered swing at the same shear stress is ~30 ms. These times are small compared to the times associated with the measured off-rates for selectins (Kaplanski et al., 1993; Alon et al., 1995a, 1997; Smith et al., 1999). This dichotomy of force and time scales indicates that there is a large difference in the contact forces and mechanics of free and tethered rolling.

Bruehl et al. (1996) have examined in detail the microvilli geometry on neutrophils (PMN), monocytes, and lymphocytes. They have also shown, by using immunogold labeling for L-selectin, that for all three cell types this adhesive protein is localized on the microvilli tips. An important feature of the microvilli geometry is their great heterogeneity in length. The average microvillus length for the three cell types falls within the narrow range of 0.3–0.4 μm, but there is a wide dispersion with a significant population (5–10%) of long microvilli (>0.5 μm in length). We will show that this small population of long microvilli is critical in initiating tethered rolling in flow chamber studies and that at shear stresses above 0.2 dyn/cm^2 short microvilli are incapable of tethering contact. At lower shear stresses contacts can be made, but the contact force may be too small for tethering attachment. We shall also demonstrate that there is an important nonlinear coupling between the weak gravita-

tional force and the hydrodynamic force in the lubricating layer which leads to a large amplification of the contact forces on the microvilli tips as the shear stress increases. This amplification depends strongly on the heterogeneity in lengths of the microvilli. One of the more intriguing questions we want to explore is the magnitude of the microvilli tip contact forces in the vicinity of the shear threshold for initial tethering. Finger et al. (1996) have demonstrated that there is no adhesive rolling for L-selectin below ~0.4 dyn/cm^2, and Lawrence et al. (1997) have observed a similar shear threshold for P- and E-selectins both in vitro and in vivo.

One of the most perplexing issues in analyzing free-rolling and initial tethering in vivo is the role of the EC glycocalyx. The latest studies (Vink and Duling, 1996; Henry and Duling, 1999) indicate that in capillaries, arterioles, and venules this surface matrix is 0.4–0.5 μm thick and composed of proteoglycans and hyaluronan, an unsulfated glycosaminoglycan. This layer thickness is approximately the same as the length of the microvilli described in Bruehl et al. (1996). If this layer provides the molecular sieve for plasma proteins that establishes the oncotic force across the microvessel wall, as hypothesized in Michel et al. (1997), Weinbaum (1998), and Hu and Weinbaum (1999), the fiber spacing of this matrix needs to be ~7 nm, i.e., the molecular dimension of albumin, which is the primary protein that determines the oncotic force. Feng and Weinbaum (Feng et al., 1998) have recently developed an effective medium theory to examine the motion of spherical particles through a porous layer of this nature. Using the diffusion data in Lee et al. (1993) for the motion of colloidal gold-tagged lipids in cells coated with a glycocalyx, they have been able to estimate both the hydraulic resistance of the particles and the binding and deformation resistance of the matrix. Several fundamental questions need to be addressed. First, how can WBCs roll along this surface glycocalyx without sinking into this highly deformable structure and grinding to a halt? The situation is akin to a human being trying to run through a snowfield whose depth is the same as his or her legs. Second, why is WBC rolling rarely observed in arteriolar capillaries, but frequently observed in postcapillary venules? Third, does the EC glycocalyx have to be enzymatically degraded to initiate tethering or are there circumstances in which the microvilli can penetrate the EC glycocalyx without degradation? A theoretical framework will be developed to examine each of these questions.

METHODS

Previous mathematical models

There is an extensive prior literature on the free rolling of WBCs as a precursor to tethered rolling and adhesion (Lawrence and Springer, 1991; Hammer and Apte, 1992; Tissot et al., 1992; Tözeren and Ley, 1992; Tempelman et al., 1994), to mention just a few of the widely cited

investigations. A consensus of these studies is that the cells roll as if they were displaced by a distance that is >500 nm from the boundaries (Tissot et al., 1992; Tempelman et al., 1994). Although it is generally believed that this displacement is due to the presence of microvilli, no study has attempted to analyze the rolling motion of WBCs with protruding microvilli or the effect of gravitational forces on the microvilli interaction, with the exception of Tissot et al. (1992). The model in Tissot et al. was developed to explain the results of their experiments on the sedimentation of WBCs at a very low shear rate of 1.3 s^{-1}. This shear rate is two to three orders of magnitude lower than the shear rates used in the great majority of flow chamber studies on cell rolling or the shear rates measured in vivo. At these low shear rates substantial sedimentation can occur between each microvillus contact. Furthermore, their idealized model considered only a single microvillus with protrusions of 0.6–1.8 μm. Their study was conducted before the publication of the extensive database of Bruehl et al. (1996) on microvillus geometry for large populations of PMN, monocytes, and lymphocytes. As noted earlier, the latter study suggests that an average microvillus has a length of 0.3–0.4 μm and a diameter of 0.1 μm. They also reported that there are typically 26 protrusions in each cell cross-section; for an 8.3-μm-diameter WBC, this corresponds to an average spacing between microvilli of ~1 μm.

The gravitational-hydrodynamic interaction problem we wish to examine involves much less sedimentation between each contact than that considered in Tissot et al. (1992). The model developed in this paper predicts that the duration of contact of a single tip collision at a shear stress of 1 dyn/cm^2 is only of the order of 1 ms. The maximum sedimentation distance in this time is only of the order of 3 nm, since the unbounded sedimentation velocity of a WBC is ~3 μm/s. At a shear stress of 1 dyn/cm^2, the time between tip contacts for equal length microvilli is about four times the duration of a grazing contact, and thus the upper bound for the sedimentation between contacts is ~12 nm. Such small displacements, although large compared to Brownian motion because of the size of the cell and the duration of contact, would seem to be of negligible importance. However, we shall show that these grazing collisions of the tips with the substrate are highly nonlinear and at a shear stress of 1 dyn/cm^2 can generate tip contact forces 20 to 100 times greater than the resting gravitational force on the tip in the absence of flow. This nonlinear amplification is of special importance in considering the penetration distance of the microvilli into the surface glycocalyx for a free-rolling cell in vivo. Without this amplification we shall show that even long microvilli would not be able to penetrate the glycocalyx and that tethered rolling would not be possible unless the surface matrix were enzymatically degraded.

Model formulation and simplification

The model formulation involves three important categories of simplification: those that involve the hydrodynamic forces and torques associated with the cell body and its microvilli, those associated with the viscoelastic deformation of the microvillus, and those that involve the presence of the surface glycocalyx through which the microvilli penetrate. We consider each separately.

The forces and torques on the WBC can be divided into two groups, those that are associated with the cell body and those that are associated with its microvilli. The hydrodynamic forces on the cell body can be calculated by approximating it as a rigid sphere, as described in the next section. Because the spacing of the microvilli is one order of magnitude greater than their diameter, and the microvillus length is one order of magnitude smaller than the cell radius, it is not necessary to include corrections for the microvilli in calculating the global hydrodynamic forces on the WBC. Similarly, corrections for lubricating hydrodynamic forces on the tips of individual microvilli in the presence of a solid boundary are not needed because these forces will be small compared to the forces on the main body of the WBC. This, however, is not true if the microvillus penetrates the glycocalyx, as the resistance in the glycocalyx is comparable to the resistance of the cell body, as discussed below.

The recent experiments of Shao et al. (1998) have provided valuable data on the time constant for achieving a full viscoelastic response of a microvillus under stretch. This time constant, 0.77 s, is nearly three orders of magnitude greater than the characteristic time, 1 ms, for the grazing contact of the microvillus tip with the surface at shear stresses typical of postcapillary venules. For forces greater than 61 pN applied over longer times, one obtains a purely viscous response in which a tether could be pulled. This viscous or viscoelastic behavior occurs on a time scale and for forces that are characteristic of tethered rolling, but not the free-rolling interaction described herein. It is also reasonable to expect that viscoelastic deformation of microvilli in compression occurs on a time scale similar to that observed for microvilli in tension. Accordingly, for the time scales in the present application, we shall treat the microvilli as being rigid, and the more important consideration is their geometric heterogeneity.

The hydrodynamic interaction of the freely rolling WBC with the porous EC glycocalyx has two components: the cell body and the microvilli. The interaction with the cell body can be considered through the use of an appropriate slip boundary condition at the glycocalyx surface, provided that the cell body is not in physical contact with the glycocalyx. The basic modification is to introduce a slip coefficient that accounts for the fluid motion through the porous layer, instead of the no-slip boundary conditions used in Brenner (1961) and Goldman et al. (1967a, b). Although more detailed theories can be developed for the motion of a sphere near a porous half-space, the basic simplification can be deduced from simple intuitive arguments derived from effective medium theory (Brinkman equation (Brinkman, 1947)). One can readily show from this equation that the effective thickness of the fiber interaction layer near the surface of the glycocalyx is of the order of $K_p^{1/2}$, where K_p is the Darcy permeability of the porous medium. The magnitude of the slip at the porous interface is proportional to the ratio $(K_p^{1/2}/\delta)U$, where δ is the thickness of the gap width between the sphere and the porous surface, and U is the sphere velocity. For a periodically ordered parallel array of fibers, Tsay and Weinbaum (1991) give a simple approximate expression for K_p

$$K_p = 0.0572a^2\left(\frac{\Delta}{a}\right)^{2.377} \tag{1}$$

where a is the fiber radius and Δ is the open space between fibers. For $\Delta = 7$ nm, which is the fiber spacing for the glycocalyx to be a molecular sieve for albumin, and $a = 0.6$ nm, which is the characteristic radius for glycosaminoglycans, one finds that $K_p^{1/2}$ is less than 3 nm. Therefore, even at a gap distance of several tens of nanometers, the slip will be very small. The no-slip condition can thus be applied with little error.

The penetration of the microvillus tip into the glycocalyx can only be treated in a much more approximate fashion at this time. Using the theory in Feng et al. (1998) and the experimental measurements in Lee et al. (1993) for the Brownian motion of colloidal gold-tagged lipids as a probe for the resistance of the surface matrix, we shall show that a 0.1-μm-diameter sphere will move through the surface glycocalyx at a velocity of ~6 μm/s under an applied force of 1 pN. This sphere is an approximate model for the normal penetration of the microvillus tip. In contrast, one can readily calculate from the Stokes formula, $F = 6\pi\mu U R_c$, that a 1-pN force applied to the entire cell body will cause it to move at a velocity of 12 μm/s in a fluid whose viscosity is 1 cP. The resistance of the microvillus tip, once it enters the glycocalyx, is thus comparable to the entire cell body. In the limit where the tip penetration is small compared to the microvillus length, the contact forces that will be calculated for the free rolling of a WBC on a solid surface will provide a good approximation for the penetration force on the microvillus tip because the displacement of the tip during contact with the glycocalyx will be small. This will be seen to be the case for microvilli of uniform length for all levels of shear stresses encountered throughout the microcirculation. However, for a heterogeneous distribution of microvilli with a small population of long microvilli, this will only be true for high fluid shear stresses typical of those found on the arterial side of the microcirculation where the tip penetration will be

shown to be small. For the low shear stresses found in postcapillary venules, a more sophisticated theoretical model needs to be developed in which the instantaneous velocity and displacement of the microvillus in the glycocalyx are taken into account in calculating the penetration forces on long microvilli. Such a theory goes beyond this initial model because it requires the consideration of the actual shape of the microvillus and its motion, both normal and parallel to the EC surface. However, the present model provides a valuable upper bound for estimating this penetration.

Model for predicting tip contact forces in a gravitational field

In view of the discussion in the previous section, we shall first formulate a hydrodynamic model for predicting the contact forces on a WBC experiencing free rolling on a solid surface in a gravitational field. This is because 1) the force of microvillus contact with a solid wall constitutes an upper bound for the contact force with an EC glycocalyx surface, and hence the predicted value can be used to estimate an upper bound for the penetration of the microvillus into the EC glycocalyx; and 2) in many WBC rolling experiments performed in flow chambers, the substrate surface is truly a solid wall.

Consider the motion of a WBC in a viscous shear flow bounded by a nearby planar wall as shown in Fig. 1. Let (x, y, z) be a right-handed system of rectangular Cartesian coordinates, of which the xy-plane coincides with the bounding wall, the x axis points in the direction of the flow, and the z axis points into the fluid normal to the wall. For simplicity we assume that the motion of the cell is constrained to the xz-plane, i.e., the cell center is always in the $y = 0$ plane and there is no rotation of the cell about the z axis. The cell, therefore, has three degrees of freedom: its motion is fully described by specifying (x_c, z_c, θ_c) as functions of time t, where x_c and z_c are coordinates of the cell center and θ_c is an angle measured from the z axis to a reference radial line fixed to the cell. Hereafter we drop the subscript c for conciseness; hence (x, y, z) will denote the coordinates of the cell center.
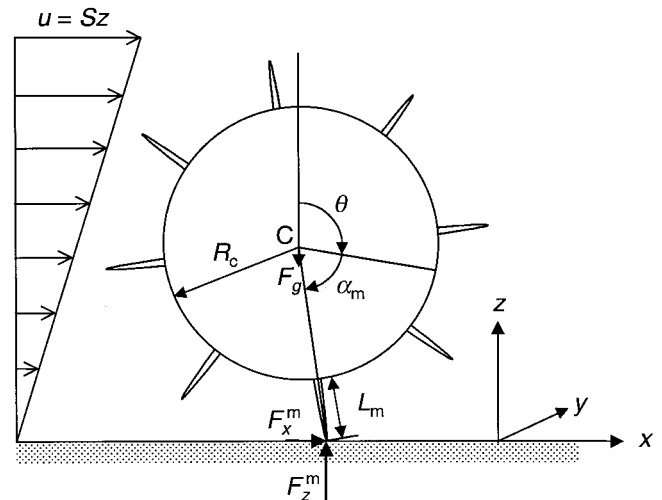

FIGURE 1 A schematic showing the coordinate system and the variables used in model formulation. The cell is modeled as a sphere decorated with surface microvilli. Its motion is assumed to be confined to the xz-plane and hence its position is fully defined by the x- and z-coordinates of its center C and the angle θ measured from the z-direction to a reference line that is fixed to the cell. Acting on the cell are gravitational force F_g (right-hand side of Eq. 5), microvillus contact force F_x^m and F_z^m, and fluid forces not shown in the schematic. See text for more detailed description.

The flow around the WBC is governed by the Stokes equation for slow viscous flow. Because of the linearity of the Stokes equation, the resultant force and torque imparted on the cell by the fluid are linear functions of the velocity components

$$v_x = \frac{dx}{dt}, \quad v_z = \frac{dz}{dt}, \quad \omega_y = \frac{d\theta}{dt} \quad (2)$$

of the cell and the shear rate S of the imposed flow. This holds for a cell of any shape. The coefficients in these linear functions will be denoted as h_i ($i = 1, 2, \ldots$) and are called hydrodynamic resistant functions. The WBC will be modeled as a sphere in the computation of the hydrodynamic forces and torques. In this case, the h_i are functions only of z, independent of x and θ.

As the cell settles in the gravitational field and rotates in the shear flow, one or more of its microvilli may make contact with the bounding wall. We assume that the contacts are momentless, i.e., a microvillus contact provides no resistance to the rotation of the microvillus tip about its contact point. In general, the contact force can be resolved into tangential and normal components, denoted as F_x^m and F_z^m, respectively. The balance of forces acting on the WBC requires

$$h_1(z)v_x + h_2(z)\omega_y + F_x^m = -h_6(z)S, \quad (3)$$

$$h_3(z)v_x + h_4(z)\omega_y + (R_c + L_m)\cos(\theta + \alpha_m)F_x^m$$
$$-(R_c + L_m)\sin(\theta + \alpha_m)F_z^m = -h_7(z)S, \quad (4)$$

$$h_5(z)v_z + F_z^m = (\tfrac{4}{3}\pi R_c^3 \Delta\rho)g. \quad (5)$$

Equations 3 and 5 are, respectively, the force balance in the x- and z-directions, and Eq. 4 is the balance of torques about the cell center. In these equations R_c is the cell radius, L_m the length of the microvillus in contact with the surface, α_m the angle measured from the reference radial line to the microvillus (and hence $\theta + \alpha_m$ is the angle measured from the z axis to the microvillus), $\Delta\rho$ the difference between mass densities of the cell and the plasma, and g the gravitational acceleration.

For a spherical cell, the hydrodynamic resistance functions h_i have been given in the literature (Brenner, 1961; Goldman et al., 1967a, b). They are given either in the form of tabulated results of numerical computation or in the form of asymptotic expressions for a sphere very close to or very far away from the bounding wall. However, in the problems of present interest, the asymptotic expressions are not applicable because the ratio of the sphere-wall gap to the sphere radius is of intermediate magnitude. The gap width is characterized by the length of the microvilli and lies in the range of 0.1–1.0 μm, while the cell radius R_c without the microvilli is assumed to be 4.15 μm. In this range of the ratio L_m/R_c, the tabulated numerical results are too scanty. Therefore, approximate expressions for h_i are used in the present computation. The approximations (see the Appendix) are derived using a method proposed by Zhao et al. (1997).

The three equations for the force and torque balance contain five unknowns, namely, the three velocity components v_x, v_z, and ω_y, and the two components of the contact force F_x^m and F_z^m. Two more equations are required to uniquely determine the cell motion. These can be obtained by considering the mode of cell motion.

Free-flowing

If no microvillus is in contact with the bounding wall,

$$F_x^m = 0, \quad (6)$$

$$F_z^m = 0. \quad (7)$$

These two equations are the standard ones for determining the translation and rotation of a sphere in a gravitation field near a planar boundary.

Free-rolling without friction

We refer to the motion of a WBC in the shear flow as free-rolling when the tip of a WBC microvillus is in contact with the bounding wall but no adhesion occurs; as the cell rotates, it swings from the upstream side of the contacting microvillus to the downstream side. As a first approximation the microvillus-wall contact can be assumed to be frictionless, i.e., Eq. 6 applies. This is a realistic assumption for a cell moving over a solid surface in which the tip contact is a grazing collision. The condition of no penetration into the solid surface imposes a constraint on the cell motion:

$$v_z - (R_c + L_m)\sin(\theta + \alpha_m)\omega_y = 0. \quad (8)$$

The contact force F_z^m is treated as an unknown. The kinematic constraint Eq. 8 is valid only if F_z^m is compressive (i.e., $F_z^m > 0$). If the computed F_z^m turns out to be otherwise, the cell motion is regarded as free-flowing, and Eq. 7 applies instead of Eq. 8.

Free-rolling with friction

In reality, a tangential force due to friction may act on the microvillus tip as it grazes the boundary surface. The magnitude of this frictional force F_x^m increases as the compressive normal force F_z^m increases:

$$F_x^m = -\eta F_z^m, \quad (9)$$

where η is the coefficient of friction. The sign in Eq. 9 is due to the fact that the frictional force F_x^m acts in the direction opposite to the sliding velocity of the microvillus tip. As the normal force increases, the frictional force may become large enough to fully arrest the sliding of the microvillus tip. If this happens, F_x^m will be smaller than that predicted by Eq. 9, and the no-slip condition at the microvillus tip requires

$$v_x + (R_c + L_m)\cos(\theta + \alpha_m)\omega_y = 0. \quad (10)$$

Hence, in the case of free-rolling with friction, Eq. 6 is no longer applicable and will be replaced by either Eq. 9 or Eq. 10, whichever predicts a smaller force of friction. By the definition of free-rolling, F_z^m is required to be compressive ($F_z^m > 0$). This requirement also indicates a difference between friction and adhesion due to bond formation: the latter involves a tensile force on the microvillus that prevents it from being lifted off the wall, while friction does not. For the case of EC glycocalyx, which we will discuss later, Eq. 9 will be applied in two limits, $\eta = 0$ and $\eta \gg 1$.

Tethered swing

When the tip of the contacting microvillus adheres to the wall, both F_x^m and F_z^m can be nonzero, and F_z^m is not necessarily compressive. The microvillus tip serves as a pivot about which the cell may rotate, and the cell motion is referred to as a tethered swing. For a tethered swing, the motion of cell must satisfy the no-penetration condition in Eq. 8 and the no-sliding condition in Eq. 10.

Given the shear rate S and the cell position, Eqs. 3–10 can be solved for v_x, v_z, and ω_y, as well as the contact forces F_x^m and F_z^m. With the values of v_x, v_z, and ω_y known, the next position of the cell can be obtained by integrating Eq. 2. The process can be repeated to yield the trajectory of the cell.

Model for microvillus penetration into the EC glycocalyx

Now, consider the possible penetration of a microvillus tip into the EC glycocalyx. The only experimental study to our knowledge that directly addresses the resistance of pericellular matrix (glycocalyx) is that of Lee et al. (1993). They measured the mobility of colloidal gold-tagged lipids in the plasma membrane of cultured fibroblasts, epithelial cells, and keratocytes. Fluorescently labeled lipids were tagged with 30-nm colloidal gold particles and the diffusional resistance of this conjugate was compared with the fluorescent lipid alone, and also after the surface glycocalyx was digested with heparinase. They found that the average diffusion coefficient of the gold-tagged lipids was only about one-fifth of that measured for the lipid molecules alone by FRAP (fluorescent recovery after photobleaching technique). The reduction in the diffusion coefficient of the gold particle was attributed to the resistance of the pericellular matrix. Note that hydrodynamic resistance is only part of the total resistance experienced by the diffusing particle or a penetrating microvillus; the rest is due to the elastic and binding energies of the fibers. Feng et al. (1998) developed an effective-medium theory based on the Brinkman equation to predict the magnitude of the hydrodynamic forces that a spherical particle would encounter if it were translating either parallel or perpendicular to a wall covered by a uniform layer of fiber matrix. They showed that when the dimensionless permeability parameter α, defined as $R/K_p^{1/2}$, is >1, as in the present case, the effects of boundaries are small because the fibers shield the particle from hydrodynamic interaction with the boundaries. Here R is the particle radius and K_p is the Darcy permeability of the porous media. In this limit the hydrodynamic resistance F_h to a sphere moving with a velocity U is given by the asymptotic expression

$$F_h = 6\pi\mu R U(1 + \alpha + \tfrac{1}{9}\alpha^2), \qquad (11)$$

which reduces to the Stokes drag for $\alpha = 0$. Feng et al. (1998) attempted to analyze the data in Lee et al. (1993), and estimated that approximately one-third of the total drag of the pericellular matrix on the gold particle can be accounted for by hydrodynamic resistance as predicted by the Brinkman equation, suggesting that about two-thirds of the total resistance is associated with the elastic and fiber binding energies of the surface glycocalyx. Using Eq. 1 and the parameter values discussed there, K_p is estimated to be 7.08 nm². For a penetrating microvillus modeled as a sphere of 0.1-μm

diameter, Eq. 11 yields a hydrodynamic resistance $F_h/U = 5.6 \times 10^{-2}$ pN per μm/s. If the total resistance F is 3 times F_h, $F/U = 0.17$ pN per μm/s. The microvillus tip would thus penetrate the glycocalyx at a velocity ~5.9 μm/s under a force of 1 pN.

RESULTS

Force and duration of microvillus contacts with a solid surface

We first consider the free-rolling interaction of a WBC with a solid surface. The contacts between WBC microvilli and the surface are assumed to be frictionless. This is realistic for many in vitro experiments in which nonspecific adhesion between the cell and surface is blocked by albumin (Zhao et al., 1995; Alon et al., 1997; Puri et al., 1998).

We start with a simple case in which 26 microvilli of equal length are distributed uniformly along the cell perimeter. Typical cross-sections of human PMN in Bruehl et al. (1996) had 26 microvilli at a frequency of 1 per 1.4 μm of plasma membrane. The mass density of PMN is ~1.08 g/ml (Schmid-Schönbein, 1987). For a sphere with a 4.15-μm radius, this corresponds to a gravitational settling force of 0.23 pN in solution and a Stokes sedimentation velocity of ~3 μm/s. Without shear flow, the load on a resting cell will be distributed among at least three contacting microvilli and the contact force at each microvillus tip would be <0.08 pN. For a cell undergoing free rolling in a shear flow, Fig. 2 shows the computed force and duration of microvillus contacts, where the mean force is a time average over the contact duration. It is interesting to note that, at wall shear stresses seen in postcapillary venules (1–4 dyn/cm²), the small gravitational settling force can lead to the generation of contact forces at microvillus tips that are 20 to 50 times

FIGURE 2 Force and duration of contact between microvilli tips and a solid wall for a cell rolling without adhesion on the wall in a shear flow. The contacts are assumed to be frictionless and the mean contact force plotted is a time average over the contact time t_c. In the computation 26 microvilli of equal length are distributed uniformly along the cell perimeter. The contact force increases nonlinearly with increasing shear stress. At wall shear stresses typically seen in postcapillary venules (1–4 dyn/cm²), a net gravitational settling force of 0.23 pN acting on the cell leads to microvilli contact forces that are many times greater, but the contacts are brief.
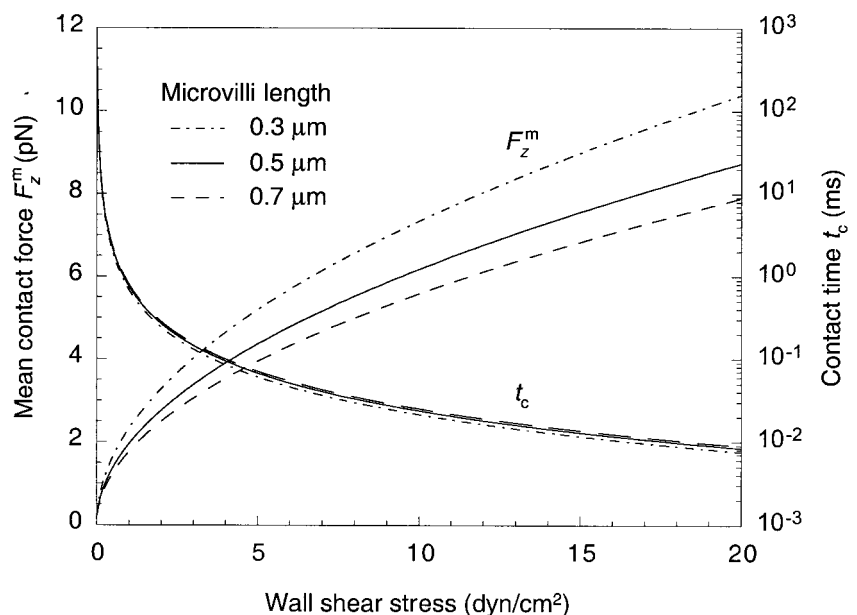
greater than the resting gravitational force of 0.08 pN cited above. However, the contacts are surprisingly brief, on the order of 0.1–1 ms. This large magnification in contact force arises from the necessity of drawing viscous fluid into a thin gap between a cell and a wall as the cell is displaced quickly from the wall following a microvillus contact. The associated viscous dissipation in the thin gap leads to a large hydrodynamic resistance to the vertical motion of the cell that must be balanced by the microvillus contact force. As the wall shear stress τ_w increases, the contact force increases approximately in proportion to $\tau_w^{0.5}$, whereas the duration of each contact decreases approximately in proportion to $\tau_w^{-1.5}$. The interesting observation that the contact duration is proportional to $\tau_w^{-1.5}$ instead of τ_w^{-1}, as one might intuitively expect, requires an explanation. The contact duration is proportional to the product of two factors. The first is the time spent by the cell to complete a single rotation. This time is barely influenced by the microvillus contacts and is expected to be proportional to τ_w^{-1}. The second is the percentage of this rotation time that is spent in actual

microvillus contact. This percentage decreases with increasing τ_w, because the increased rotational velocity of the cell reduces the time available for the settling of the cell between microvillus contacts. Therefore, the contact duration varies as $\tau_w^{-(1+a)}$, with $a > 0$. It can also be shown that, for a cell with uniform microvilli, the contact force varies in proportion to τ_w^a. For the case shown in Fig. 2, the computation indicates that the value of the constant a is ~ 0.5. The contact force is a weak function of the microvillus length, decreasing with increasing L_m, while the contact duration is essentially independent of the microvillus length.

In reality, the length of WBC microvilli has a wide distribution, ranging from <0.1 μm to >1 μm (Bruehl et al., 1996). For human PMN, the average microvillus length is 0.29 μm and 95% of the microvilli are <0.53 μm (Bruehl et al., 1996). To assess the effects of this heterogeneity in microvillus length, we consider the motion of a cell with eight microvilli uniformly distributed along its perimeter: seven of them (2–8) are 0.3 μm long, and one (1) is 0.5 μm (Fig. 3 A). The peak contact forces at the tips of both the
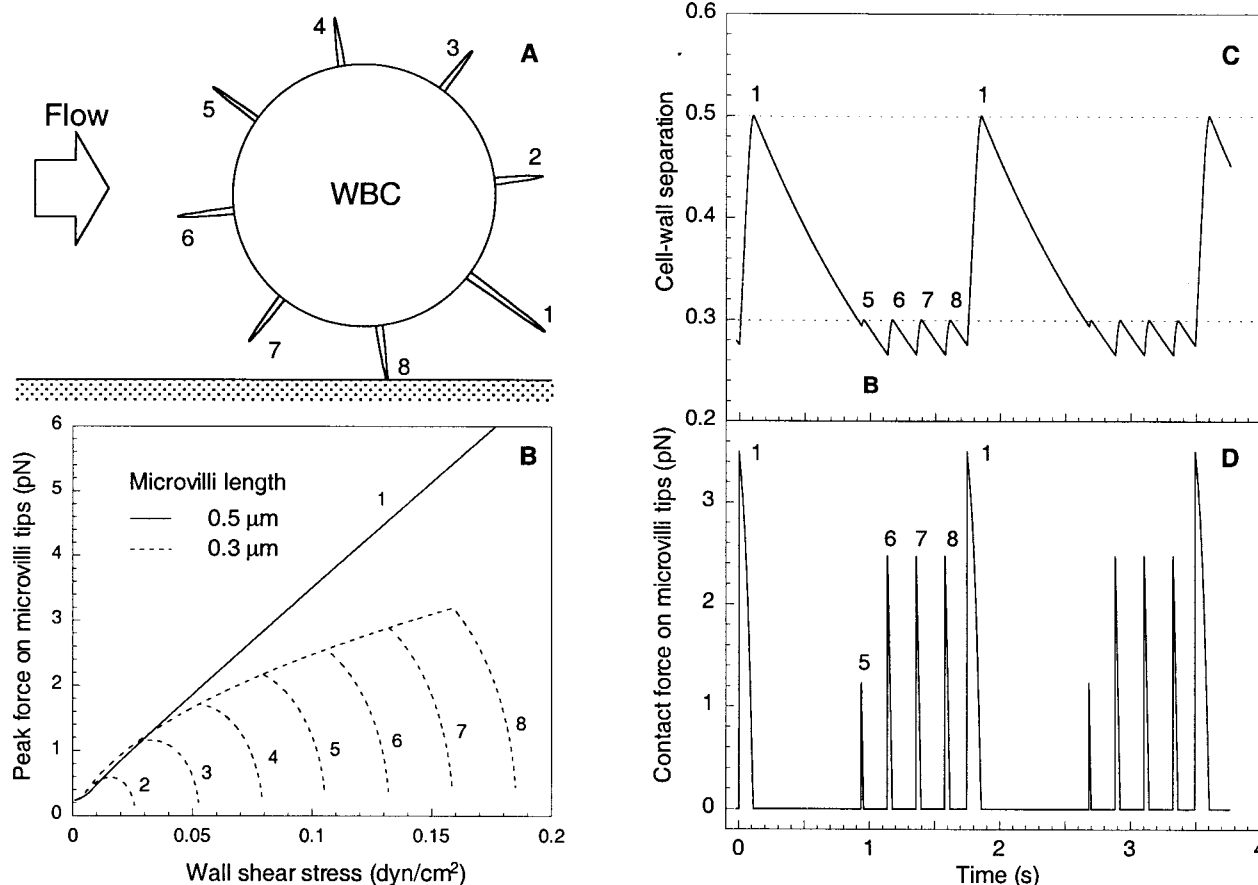

FIGURE 3   Effects of heterogeneity in microvilli length. (A) A schematic showing a WBC with one long microvillus (1, 0.5 μm) and seven shorter ones (2–8, 0.3 μm). (B) In the presence of a long microvillus (1, 0.5 μm), the shorter ones (2–8, 0.3 μm) can only touch the wall at shear stresses much lower than the shear stress threshold for selectin-mediated rolling adhesion ($\sim$0.4 dyn/cm^2 for L-selectin), suggesting that only a small population of long microvilli are effective in initiating WBC adhesion in shear flow. (C) and (D) show the dynamics of microvilli-wall interaction at 0.1 dyn/cm^2.

short and long microvilli are plotted in Fig. 3 *B*, from which it can be noted that the short microvilli make no contact with the boundary surface at $\tau_w > 0.2$ dyn/cm². The number of short microvilli is thus unimportant for initial cell-wall contacts at wall shear stresses typically seen in postcapillary venules. After being lifted by the long microvillus, the cell must settle at least $0.5 - 0.3 = 0.2$ μm to allow the short microvilli to make any contact. Increasing the shear rate increases the angular velocity of a flowing cell. At $\tau_w \gtrsim 0.2$ dyn/cm², the cell rotates too fast and the time between two successive contacts of the long microvillus becomes too short for the cell to settle the 0.2 μm necessary for the 0.3-μm microvilli to make contact. The motion of the cell becomes equivalent to that of a cell with a single long microvillus. This can be seen in Fig. 3 *C*, which shows the trajectory of the cell center at $\tau_w = 0.1$ dyn/cm². Even at this lower shear stress, the first three short microvilli (2–4) next to the long one are not able to make contact because the cell has not settled enough after the previous lifting by the long microvillus. The next one (5) barely makes a contact, and the other three (6–8) make full contacts. The contact force as a function of time is shown in Fig. 3 *D*. Note that, even at such a low shear stress, the contact time of a short microvillus is much shorter than that of the long microvillus.

The mean force and duration of the contact of the long microvillus with a solid surface are plotted in Fig. 4 as functions of wall shear stress. In the computation, 26 microvilli are distributed uniformly along the cell perimeter. All of the 25 shorter microvilli are 0.3 μm long, and the one long microvillus is 0.5 or 0.7 μm in length. Both the force and duration of contact are increased in comparison with the corresponding values shown in Fig. 2 for a WBC with microvilli of equal length. This is because a cell with microvilli that are heterogeneous in length is able to settle more between successive contacts than a cell with microvilli of equal length. For the long, 0.5-μm microvillus in Fig. 4, the mean contact force and contact time at a typical venous wall shear stress of 2 dyn/cm² are 14 pN and 1.4 ms, respectively; the corresponding values for the case of homogenous 0.5-μm microvilli are 2.8 pN and 0.27 ms (Fig. 2). These increases in contact force and duration may increase the probability of microvillus adhesion.

Swing of a tethered cell and its motion after release

That increasing the force and duration of microvillus contact helps to increase the probability of microvillus adhesion is a concept that is not only intuitively appealing, but also useful in interpreting experimental observations that have not been well explained. First, let us consider a situation in which a cell is tethered at a single point (presumably at a microvillus tip) in a shear flow. When the direction of flow is suddenly reversed, the cell will swing from one side to the other. This is the tethered swing mentioned in Methods. In this case the effects of the gravitational force are negligible and the swing velocity is proportional to shear rate, and hence the wall shear stress τ_w. The components of cell velocity at $\tau_w = 1$ dyn/cm² are plotted in Fig. 5 *A* as a function of time and microvillus length. The length of the microvillus has been assumed to be constant during the swing. This is reasonable because the microvillus is unlikely to be stretched, as the duration of the swing (<40 ms, Fig. 5 *A*) turns out to be much shorter than the characteristic time of viscoelastic extension of a WBC microvillus, 770

FIGURE 4   Contact force and duration as functions of wall shear stress for the long microvillus (0.5 μm) shown in Fig. 3 *A*. Results for a longer microvillus 0.7 μm in length is also shown for comparison. Compared to the results for homogeneous microvilli length shown in Fig. 2, the force is greater and the duration is longer at every shear stress. Increases in contact force and duration would help to promote initial tethering of WBC in shear flow.
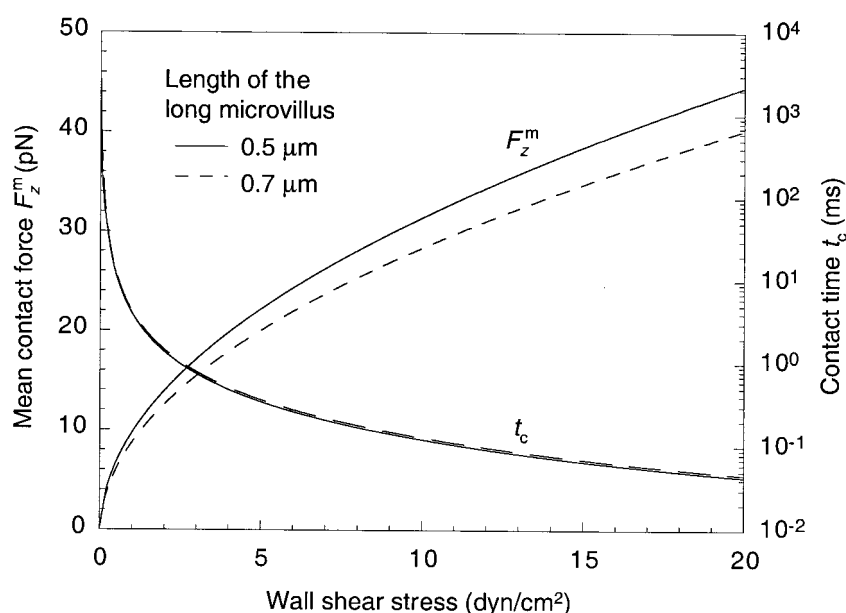
FIGURE 5 (*A*) Computed velocity of a cell tethered at a single point. The cell swings as a flow of 1 dyn/cm² is reversed. The tether is unlikely to be stretched because the duration of swing is much shorter than the characteristic time for WBC microvillus extension, 770 ms (Shao et al., 1998). (*B*) The mean swing velocity is a function of the initial cell-wall gap width; the swing starts from the initial cell-wall gap width (abscissa) and ends in the computation at a gap width 0.3 μm at the other side of attachment point (see text). For average swing velocity to agree with the experimental measurements of Alon et al. (1997), the initial effective gap width is found to be ~10–15 nm, depending on the tether length, and is ~13 nm for a 0.7-μm tether.
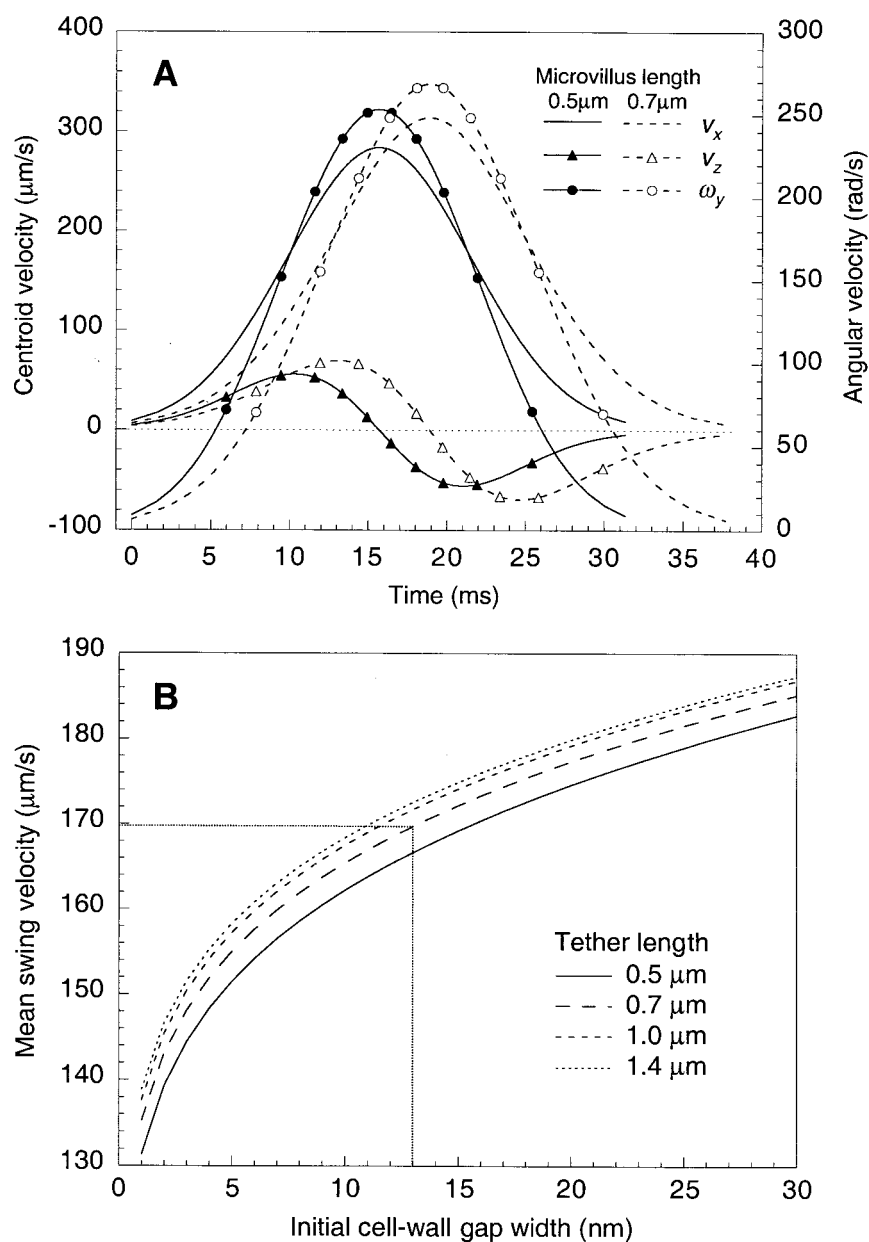
ms (Shao et al., 1998). This observation is consistent with the experimental finding (Alon et al., 1997) that the swing distance is independent of τ_w from 0.3 to 0.8 dyn/cm².

At the time of flow reversal, the cell is tethered and hence pressed by the shear flow against the substrate surface for a time characterized by the lifetime of adhesion bonds, which can be on the order of 1 s for selectin bonds (Alon et al., 1995b; Zhao et al., 1995; Puri et al., 1998), a time comparable to the characteristic time (770 ms) of the WBC microvilli's viscoelastic deformation (Shao et al., 1998). Therefore, microvilli immediately below the cell center could have been compressed into the cell body, and the swing could start from a cell-surface gap width that is much smaller than the microvillus length. However, the fast swing

shown in Fig. 5 *A* takes <40 ms, which is comparable to the swing time measured by Alon et al. (1997). Only a small fraction of this swing time will be available for compressing microvilli and the cell body at the end of the swing. Significant deformation of WBC microvilli could, therefore, only happen after this fast phase of swing is completed. Compression would occur over a time that is much longer than the 40-ms swing time. We therefore assume that the fast phase of swing ends at a gap width corresponding to the average length of WBC microvilli, namely 0.3 μm. Now, let δ denote the effective cell-surface gap width (in the sense of hydrodynamic interaction) from which the swing starts, i.e., at the time the flow is reversed. The mean velocity of the fast swing, calculated as the cell displacement in the flow

direction divided by the time of the swing, can be calculated and the results are shown in Fig. 5 *B*. Comparing the results of this computation with the measurements of Alon et al. (1997) indicates that δ is ~10–15 nm, depending on tether length, and is ~13 nm for a 0.7-μm tether. This extremely small value of δ (smaller than the length of P-selectin) suggests that before the reversal of flow, the cell body immediately below the cell center might be flattened, leading to a decrease in the curvature of the cell body in a local region where thin-film lubrication effects dominate the resistance of the cell body in lifting off from the surface.

Shown in Fig. 6, *A* and *B* are the normal and tangential tethering forces during the fast phase of swing at $\tau_w = 1$ dyn/cm². The swing starts from an effective cell-surface gap width of δ = 13 nm, and ends at a gap width of 0.3 μm at the other side of the point of tethering. Following this fast phase is the slow phase of the swing, during which the microvilli immediately below the cell center are compressed to deform viscoelastically. The cell velocity during the slow phase will be negligibly small in comparison with the velocity during the fast phase, and the force acting at the tether will be essentially the tethering force acting on a stationary cell, which is indicated by the filled symbols (Fig. 6 *A*) or dashed line (Fig. 6 *B*) for comparison.

FIGURE 6 Dynamic tethering forces during a swing at 1 dyn/cm². (*A*) Normal force. (*B*) Tangential force. The swing starts from an initial cell-wall gap width of 13 nm. The fast phase of swing (*solid lines*) ends at a gap width of 0.3 μm. Afterward, the cell deforms viscoelastically and its velocity will be negligibly small; hence, the tethering force will approach (*dashed arrows*) the value for a stationary cell that is indicated by filled symbols for normal force (*A*) and a dashed line for tangential force (*B*).
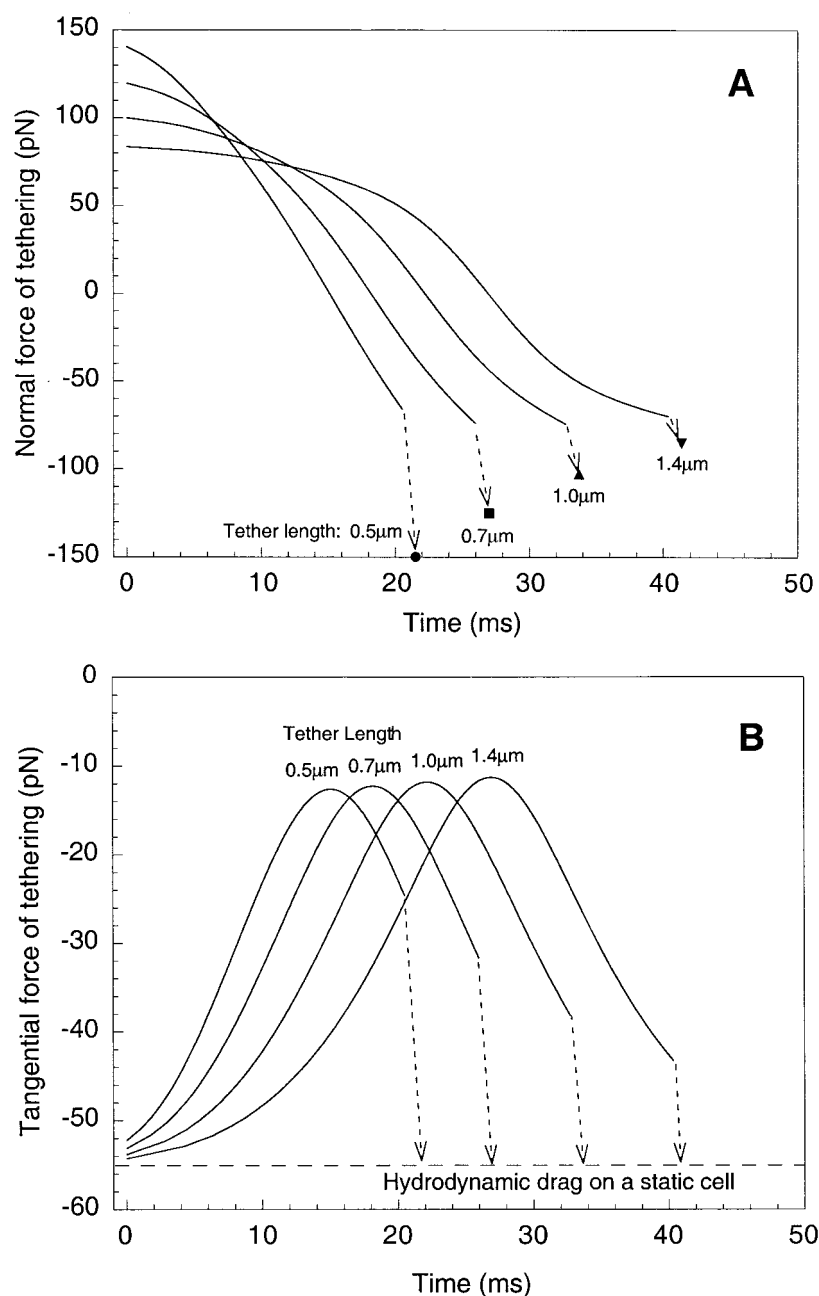
Now, consider the adherent rolling of WBC on a solid surface in a flow chamber. It is expected from the stochastic nature of the rolling adhesion (Zhao et al., 1995) that, occasionally, the rolling cell may momentarily detach from the surface. This behavior is frequently observed for rolling adhesion around a shear stress threshold (Lawrence et al., 1997). To maintain the adherent rolling, the cell must reattach immediately. One therefore expects that the probability of a tethering contact immediately following cell detachment will be much greater than that for the initial tethering of a freely flowing cell. Using results from Fig. 5 B, it is reasonable to assume that the effective cell-surface gap width δ for a newly detached cell is ~10–15 nm. As the detached cell rotates, the first microvillus downstream of the original cell-surface contact region will lift the cell from the surface, starting from a small gap width that is taken in this case to be 13 nm. The length of this microvillus is most likely to be ~0.3 μm, the average length of WBC microvilli. The ratio of the mean contact force at the tip of this 0.3-μm microvillus to that at the tip of the 0.5- or 0.7-μm microvillus shown in Fig. 4 for a free rolling cell of heterogeneous microvillus length is plotted in Fig. 7 A. Plotted in Fig. 7 B is the corresponding ratio for the contact time. It can be seen that both the force and time of contact are much greater in the case of immediate reattachment, and the ratios increase with increasing wall shear stress. At the threshold shear stress 0.4 dyn/cm^2, both the mean force and time of contact are enhanced by >3-fold. At 4 dyn/cm^2, the enhancements are 9–12-fold.

Interaction of WBC microvilli with the EC glycocalyx

As a first approximation, the glycocalyx can be regarded as a linear medium through which a particle will move at a velocity proportional to the driving force. Therefore, the depth of penetration by a microvillus into the glycocalyx will be proportional to the product of the mean contact force and the contact time. It has been estimated in Methods that a 1-pN force will drive a microvillus tip of 0.1-μm diameter into the EC glycocalyx at a velocity of 5.9 μm/s. This allows us to estimate the penetration depth of microvilli from the computed contact force and duration. Fig. 8 shows the estimated penetration depth for the case of 26 microvilli of homogeneous length. The estimation is based on our calculation shown in Fig. 2 for the contact force and time on a solid surface with the assumption of frictionless contact. If the frictional force on the microvillus tip on the EC glycocalyx is negligible, the penetration force predicted will be an upper bound because the glycocalyx dissipates the upward thrust of the microvillus on the cell body. However, if the penetration depth of the microvillus is small compared to the height of the upward swing, the force predicted for contact with a solid surface will be a good approximation. For the cases shown in Fig. 8 the penetration depth is

approximately inversely proportional to the wall shear stress τ_w. The penetration depth is insensitive to the microvillus length. At τ_w = 0.2 dyn/cm^2, the calculated penetration depth is 43 nm for 0.5-μm microvilli. However, this penetration depth falls to 4 nm at τ_w = 2 dyn/cm^2, and to <1 nm at shear stresses >10 dyn/cm^2.

The penetration predicted in Fig. 8, though small in the sense that the integrity of the glycocalyx is not compromised, may induce resistance to the tangential motion of the microvillus tip. This resistance can be accounted for through the use of the friction coefficient η defined in Eq. 9. Fig. 9 shows the contact forces at the tip of a 0.5-μm microvillus at a wall shear stress of 2 dyn/cm^2, where η = 0 corresponds to a frictionless contact and η = 20 a contact of essentially infinite friction. That η = 20 is essentially an infinite value is indicated by the abrupt drop of the frictional force F_x^m at the end of the contact. A more realistic value of η for small tip penetration is 0.2. As shown in Fig. 9, the difference in the normal force of contact (F_z^m) between η = 0 and 0.2 is quite small, and hence the approximation of frictionless contact used in Fig. 8 is reasonable for the free-rolling interaction of a WBC with the EC glycocalyx, as long as the penetration depth is small.

The limiting cases, η = 0 and 20, bracket the resistance to the tangential motion of the microvilli through the EC glycocalyx. To estimate the force of penetration for the long microvillus in the heterogeneous case, forces of microvillus contact with a solid surface were calculated for both limiting values, η = 0 and η = 20. The time-averaged normal component of the contact force F_z^m and the duration of contact t_c are plotted in Fig. 10. The normal force is increased by approximately one-third due to the presence of friction. However, the contact time is decreased by friction; this is because the frictional force resists the sliding of microvillus tip on the surface and hence the cell, which is pushed by the shear flow, is forced to rotate faster than without friction.

It turns out that the impulse $F_z^m \times t_c$, and hence the estimated penetration depth into glycocalyx, is nearly independent of friction coefficient η. The estimated depth of penetration by the long microvillus into the EC glycocalyx is plotted in Fig. 11 as a function of wall shear stress. The penetration depth is not sensitive to the friction coefficient or to the length of the microvillus. The penetration depth is much greater for heterogeneous microvilli (Fig. 11) than for microvilli of equal length (Fig. 8). The calculation indicates that the long microvillus in the heterogeneous case might be able to completely penetrate the EC glycocalyx at τ_w < 0.5 dyn/cm^2, provided that interference from the contact interactions of shorter microvilli with EC glycocalyx are neglected.

DISCUSSION

The present results provide new insights into several problems in WBC rolling and tethering dynamics that have not

FIGURE 7 Microvillus contact force (F_z^m reattachment) and contact time (t_c reattachment) associated with the reattachment of a recently detached adherent cell are greater and last longer than for a free-rolling cell. It is assumed in the computation that the reattachment contact starts from a 13-nm initial effective cell-wall gap width (Fig. 5) and the contacting microvillus is 0.3 μm long. The reattachment contact of this 0.3-μm microvillus is compared with the free-rolling contacts shown in Fig. 4, in which the microvillus length is either 0.5 μm (*solid lines*) or 0.7 μm (*dashed lines*). (*A*) Contact force ratio. (*B*) Contact time ratio.
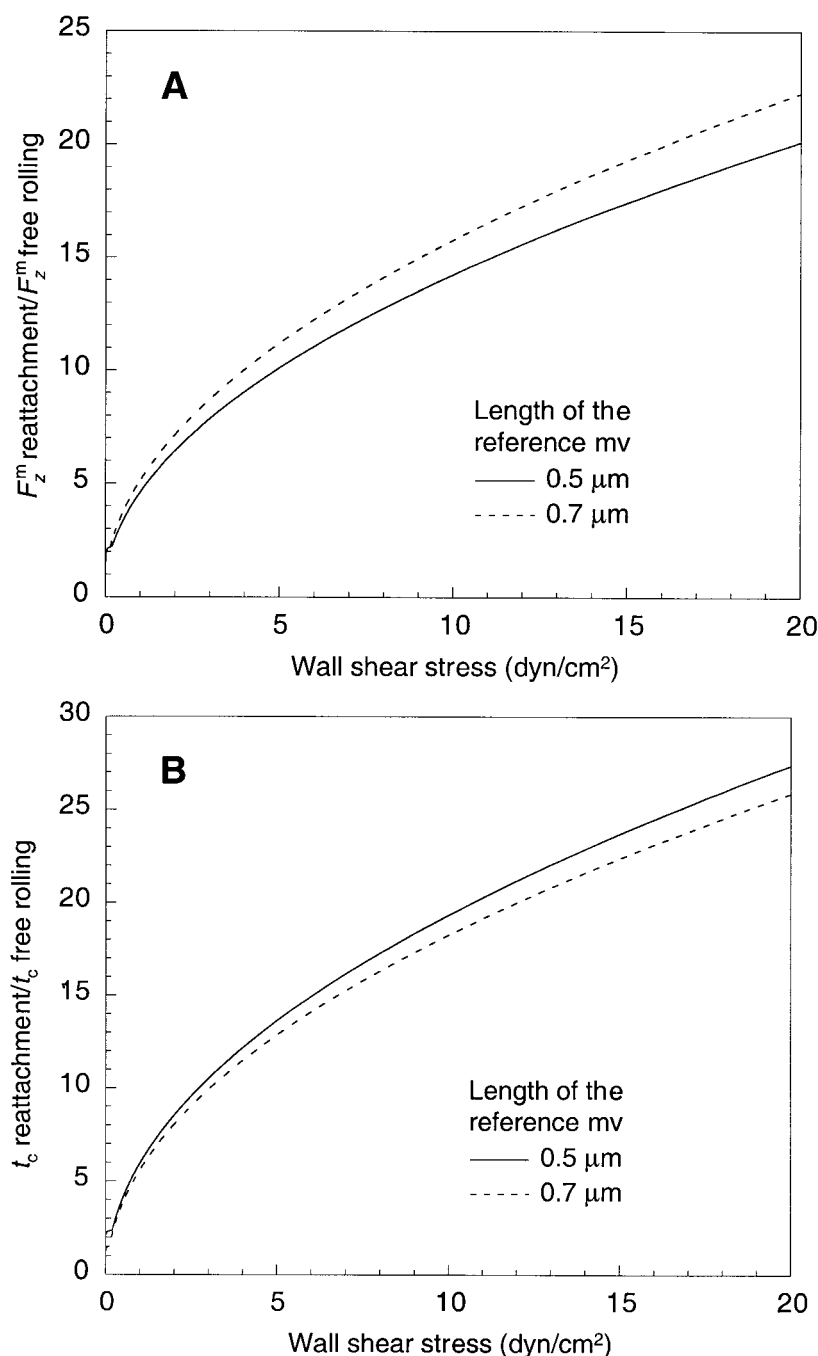
been well understood. We shall examine the implications of our results in WBC rolling and tethering dynamics in the following order: 1) free rolling on solid substrates with and without friction; 2) the shear stress threshold phenomena for L-, P-, and E-selectins; 3) tethered swings on solid substrates; 4) free rolling and the penetration of the EC glycocalyx; and 5) tethered rolling in vitro and in vivo.

Although all flow chamber studies have been conducted in a gravitational field, the effect of gravity has often been neglected because the sedimentation force on a WBC (0.23 pN) or on an individual microvillus (<0.1 pN) is three orders of magnitude smaller than the static forces on the microvilli during pauses in tethered rolling at shear stresses typically found in postcapillary venules. It thus seemed reasonable that the grazing contacts in free rolling would produce contact forces that are not very different from sedimentation forces. The one study where the effect of gravity was striking was the inverted flow chamber experiment in Lawrence et al. (1997). In this experiment the rolling of HL-60 myelocyte cells on P- and E-selectins were

FIGURE 8 Penetration of microvilli into EC glycocalyx for a free-rolling WBC with microvilli of equal length. Penetration depth is calculated from the contact force and duration shown in Fig. 2 and a penetration velocity of 5.9 μm/s per 1-pN driving force estimated in Methods.
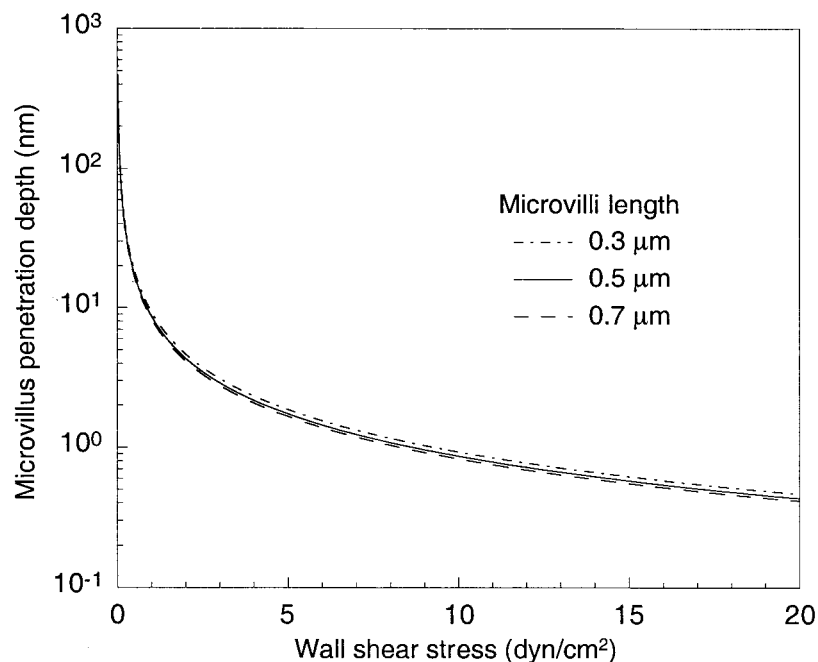
examined after the flow chamber was inverted. At a shear stress of 1 dyn/cm^2, cells were able to roll for several minutes after the inversion of the chamber, but at a shear stress of 0.1 dyn/cm^2 nearly all cells detached within 15 s. The critical rolling velocity at this low shear stress is ~30 μm/s. It was hypothesized that a cell released after tethering adhesion would have sufficient time to fall away from the top surface to prevent the reattachment of another microvillus. The feasibility of this hypothesis will be quantitatively examined below. The shear stress 0.1 dyn/cm^2 was also

significantly below the threshold shear stress of 0.5 dyn/cm^2 where the tethering to P- and E-selectins was maximized.

What has not been previously appreciated is the highly nonlinear amplification that results from the coupling of hydrodynamic and gravitational forces in the free-rolling interaction. This coupling leads to microvilli contact forces that greatly exceed gravitational forces even for grazing contact. This is illustrated in Fig. 2 for a WBC with microvilli of homogeneous length, where it is observed that contact forces increase very rapidly as a function of shear

FIGURE 9 Effects of friction on the force and duration of microvillus contact. Frictional contacts are governed by Eqs. 9 and 10. The normal (solid lines) and tangential (dashed lines) components of the contact force are shown for two limiting cases ($\eta = 0$ for a frictionless contact and $\eta = 20$ for a contact that essentially prevents any slip) and an intermediate case ($\eta = 0.2$) characteristic of small penetration depth.
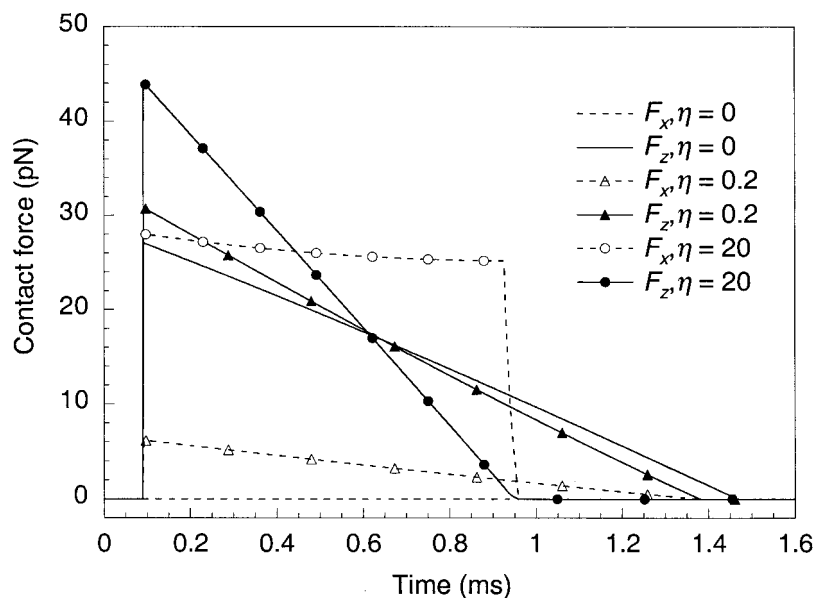
FIGURE 10 Force and duration of microvillus contact with a solid surface with and without friction. The two limiting values of friction coefficient, $\eta = 0$ and $\eta = 20$, are used to bracket the resistance to the tangential motion of a microvillus through EC glycocalyx. Shown here are the time-averaged normal component of contact force at the tip of a long microvillus and the contact time; short microvilli do not make contacts at wall shear stress >0.2 dyn/cm². The presence of friction increases the normal force but reduces the duration of contact.
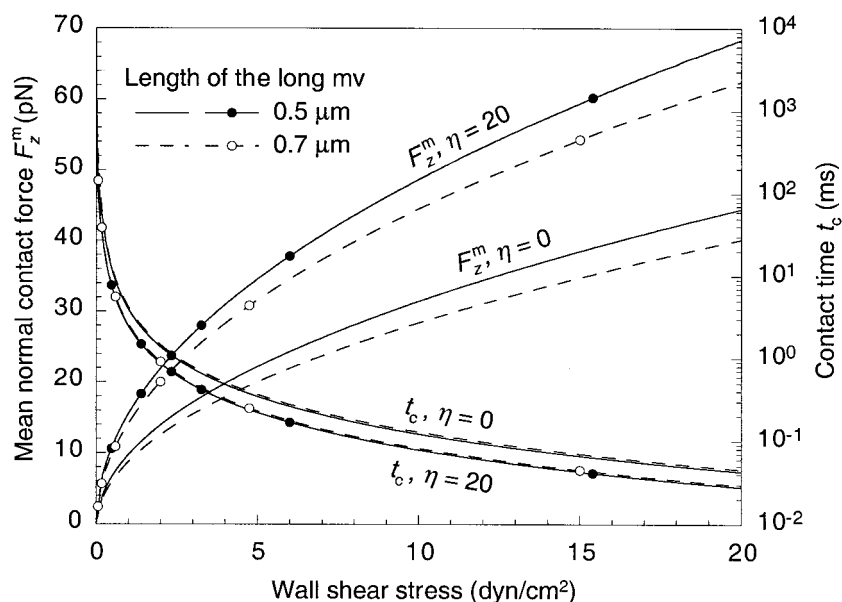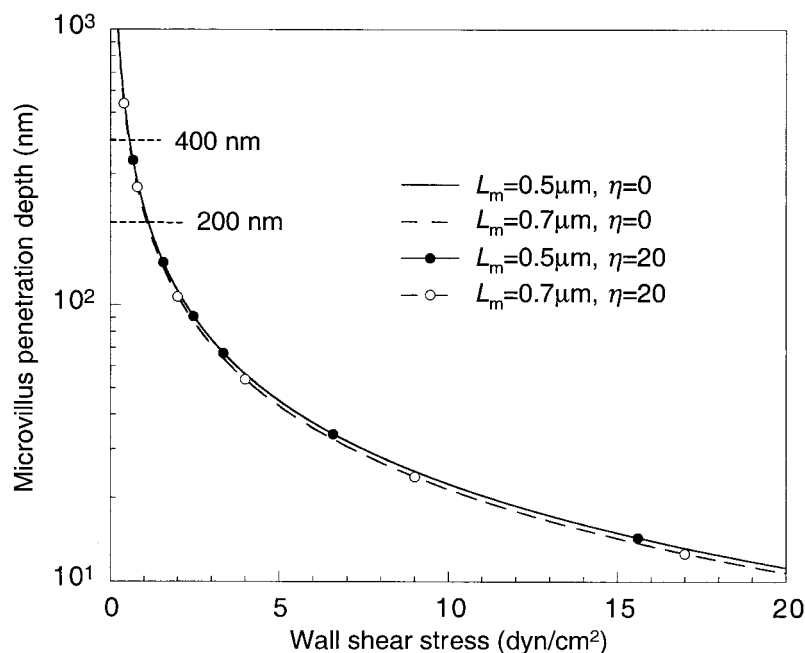
stress and that at a shear stress of 1 dyn/cm² the average contact force is nearly 20 times greater than the sedimentation force. Furthermore, Fig. 4 shows that this contact force amplification is greatly enhanced for heterogeneous microvilli and that for a single long microvillus this amplification is nearly 100-fold at a shear stress of 1 dyn/cm².

A second important feature of free rolling is the role of heterogeneity in microvillus length at low shears. Fig. 3 shows that, even if only a single long microvillus is present, it is unlikely that contact will ever be made with shorter microvilli for shear stresses > ~0.2 dyn/cm². This is due to

the large increase in hydrodynamic resistance of the lubricating layer between the cell body and the wall for gap distances comparable to a typical microvillus length. When the gap height is <0.5 μm the sedimentation velocity will decrease >10-fold. This is evident from the results in Fig. 3 C, which show the change in cell-wall separation as a function of time. In the inverted flow chamber experiment in Lawrence et al. (1997) cited above, the cell will be moving away from the wall due to gravity. By examining the magnitude of the saw teeth in the curves for the cell-wall separation, one concludes that the cell will sediment ~0.2

FIGURE 11 Penetration of a long microvillus into EC glycocalyx for a free-rolling WBC with microvilli that are heterogeneous in length. Penetration depth is calculated from the normal contact force and duration shown in Fig. 10 and a penetration velocity of 5.9 μm/s per 1-pN driving force, as estimated in Methods. The difference in calculated penetration depth due to the presence of friction is too small to be seen because of the line thickness. Interference from the contact interaction of short microvilli with the EC glycocalyx, which will occur at penetration depth indicated by the horizontal dashed lines, are not included in the computation.

μm over half a revolution at a shear stress of 0.1 dyn/cm^2, and that one revolution of the cell takes just under 2 s. This implies that if a cell is released from a 0.3-μm microvillus it will be unable to make contact with a 0.5-μm microvillus if the latter is more than half a rotation away. This accounts for the rapid dropoff in the number of rolling cells in the inverted flow chamber experiment, as Lawrence et al. (1997) hypothesized.

The foregoing results have important implications for the shear threshold that Finger et al. (1996) have observed for L-selectin and Lawrence et al. (1997) have observed for P- and E-selectins. The former occurs at a shear stress of 0.4 dyn/cm^2, whereas some tethering adhesion occurs for E- and P-selectin at lower shear stresses. First, it is clear that at these shear stresses only the longest microvilli will ever make contact with the seeded ligand substrate, since Fig. 3 shows that microvilli of average length will rarely be accessible at shear stresses above 0.2 dyn/cm^2 because of the greatly retarded sedimentation at these cell-wall separation distances. Second, at shear stresses below 0.2 dyn/cm^2 where sedimentation can allow for contact, the contact forces are <1 pN (see Fig. 2). In contrast, the contact force on a long 0.5-μm microvillus is ~6 pN (Fig. 4) at this same shear stress. Although there have been extensive studies on the kinetics of tether bond dissociation for L-, P-, and E-selectins (e.g., Kaplanski et al., 1993; Smith et al., 1999), there has been no equivalent study of the kinetics of tether bond formation. The present model predictions suggest that this kinetics may be determined by the contact force. Figs. 2 and 4 clearly show that the contact time grows exponentially with decreasing wall shear stress at very low shear, and that the contact force on a microvillus rapidly approaches the contact force of a stationary cell in a gravitational field, which we have estimated to be <0.1 pN. The studies on shear threshold for the selectin-mediated rolling adhesion (Finger et al., 1996; Lawrence et al., 1997) have indicated that frequency of tethering is much lower at very low wall shear stresses than at the threshold shear stress. Because greatly reduced tethering is observed for even greatly prolonged contact times at very low shear, bond formation appears to require a minimum force of contact that significantly exceeds the gravitational sedimentation force. Thus, the rate constant of bond formation seems to be a strongly increasing function of the contact force until the rate constant reaches a plateau. This behavior could be due to an increase in the receptor-ligand encounter rate as the contact force increases, because an increase in the contact force helps to overcome the repulsion between the two opposing surfaces and may also flatten the microvillus tip and increase the area of contact. After the rate constant of bond formation reaches its plateau, further increases in the wall shear stress will reduce the apparent rate of bond formation due to the reduction in microvillus contact time.

The duration of contact in a free-rolling interaction is remarkably short. At shear stresses found typically in post-

capillary venules, e.g., 2 dyn/cm^2, the duration of contact for a WBC with equal-length microvilli is ~0.2 ms and nearly independent of the microvillus length (see Fig. 2). As shown in Fig. 4, this contact time can increase to ~1 ms for a long microvillus. Both times are more than two orders of magnitude shorter than the viscoelastic time constant measured in Shao et al. (1998), 770 ms. Though the experiments by Shao et al. were conducted for stretch rather than compression or bending, it seems quite reasonable to assume that the microvilli on this very short time scale behave as stiff bristles.

Is a 1-ms contact long enough to promote microvillus tethering? For surface-bound selectins and selectin ligands, a reasonable estimate for the rate constant of bond formation is 0.6 μm^2/s (Tözeren and Ley, 1992), which was deduced from experimental data reported for P-selectin binding. The probability of forming at least one bond upon a microvillus contact is approximately this rate constant multiplied by the ligand density on the substrate surface (~100 μm^{-2}, Puri et al., 1998), the number of receptors at the microvillus tip (~10, Bruehl et al., 1996), and the microvillus contact time, provided that the resulting probability estimate is small. Therefore, the probability for a 1-ms contact leading to a tether event could be as high as (0.6 μm^2/s) · (100 μm^2) · (10) · (10^{-3} s) = 0.6. This order-of-magnitude estimate indicates that the amazingly short microvillus contact time is reasonable in light of what is currently known about the values of parameters for selectin-mediated rolling adhesion.

The forces and the characteristic times for a tethered swing in Figs. 5 and 6 are more than an order of magnitude greater than the corresponding forces and times that have just been discussed for free rolling at the same fluid shear stress. The principal cause of this difference is the near contact with the wall that can be achieved during a tethered swing. As shown in Fig. 5 B, the model predicts that the mean swing velocity measured in Alon et al. (1997) can be achieved if the cell starts from a separation that is ~10–15 nm from the wall. This implies that the microvilli in the vicinity of the near contact have been greatly compressed, as this separation distance is small compared to the length of the microvillus. The measured elastic constant for microvillus stretch is 34 pN/μm (Shao et al., 1998). Because this constant should be nearly the same for stretch and compression and the normal contact forces on the attaching tether are of the order of 100 pN (see Fig. 6), it is realistic to expect large compressions of the microvilli in the equilibrium state at the start of a swing.

At a shear stress of 1 dyn/cm^2, the duration of the tethered swing is <40 ms. Although this time is one to two orders of magnitude greater than the contact times for free rolling, it is still short compared to the viscoelastic time constant, 770 ms, for tether elongation measured in Shao et al. (1998). Therefore, the microvillus can, to a first approximation, be treated as being rigid when considering swing dynamics,

whereas in the equilibrium state at the beginning or end of the swing there will be a slow relaxation in which the tether will elongate to decrease the tensile force on the adhesive bonds, as proposed in Shao et al. (1998). The inelastic behavior for the dynamics of the swing is supported by the observations in Alon et al. (1997), which reveal that the swing distance is nearly independent of shear stress in the range $0.3-0.8$ dyn/cm^2.

In Fig. 9 the model for the penetration of the EC glycocalyx during free rolling was examined in two limits that should bracket the behavior that would be anticipated if a more accurate model could be constructed for the anisotropic resistance that is encountered by the motion of the microvillus tip. One limit is the case where the tangential force vanishes, $\eta = 0$, and the other is the case where the contact friction is so great that the lateral displacement of the tip is negligible, $\eta = 20$. The results shown in Fig. 9 are for a shear stress typical of postcapillary venules, 2 dyn/cm^2, but they can be scaled to any other shear stress using the results in Fig. 10. The effect of frictional resistance is to shorten the duration of contact by about one-third and increase the normal contact force on the microvillus tip by about one-third between the two limiting cases. Friction increases the rotation velocity of the cell because it reduces the slip, and hence increases the contact force because the cell is lifted more quickly from the surface. For a WBC undergoing free rolling on a solid substrate, where a reasonable estimate for the coefficient of friction is $\eta = 0.2$, Fig. 9 shows that there would be only a small deviation from the tangential slip conditions that have been used to describe the grazing contact forces in flow chamber studies that we have already discussed.

For microvilli of uniform length, Fig. 8 shows that the predicted depth of penetration is remarkably small at shear stresses typical of postcapillary venules and that this penetration depth is essentially independent of microvillus length. At a wall shear stress of 2 dyn/cm^2 the penetration depth of the microvillus tip is ~4 nm or a tenth of a microvillus radius. This insignificant penetration justifies the simplifying assumption we have made in using solid boundary analysis to predict the contact forces on the microvillus tips. The effect of friction in this case would also be very small in absolute terms. The WBC is literally tip-toeing on the EC glycocalyx, much like the Jesus Christ lizard can run across water. The situation for heterogeneous microvilli is significantly more complex. At fluid shear stresses typical of the arterial side of the circulation, i.e., $10-20$ dyn/cm^2, the penetration depth for a long microvillus is still quite small, ~$10-20$ nm, compared to the estimated thickness of the EC glycocalyx in Henry and Duling (1999), i.e., $0.4-0.5$ μm. This suggests that it would be very difficult for WBC to initiate adhesive rolling on the arterial side of capillaries, except in regions of low shear or flow reversal, unless there is a highly localized enzymatic degradation of the EC glycocalyx, e.g., due to inflammation. The situation at low shear is markedly different. The results in Fig. 11 indicate that penetration depths of 100 nm or more are readily possible for shear stresses below 2 dyn/cm^2. The model also predicts that this penetration is relatively insensitive to the friction coefficient because friction decreases the contact time, but increases the contact force, and it is the product of the two, or the impulse, that determines how far the microvillus tip will penetrate.

It should be noted that the gravitational force is the only force of margination included in this computation. In the microcirculation, shear-induced margination force due to the presence of red blood cells (Chien et al., 1984) will also play a role in bringing WBCs closer to the vessel wall between successive microvilli contacts, and hence increasing the force, duration, and penetration depth of microvillus-glycocalyx contacts. Because the shear-induced margination force is a function of shear rate (hence wall shear stress), in contrast to the constant gravitational force, the decrease in penetration depth with increasing wall shear stress shown in Fig. 11 could be significantly offset by shear-induced margination forces.

The foregoing predictions provide new understanding as to the quantitative feasibility of tethered WBC rolling in postcapillary venules in vivo and its relative absence in arterioles and arteriolar capillaries. The results predict that at low shear stresses typical of postcapillary venules, the WBC microvilli can readily penetrate the EC glycocalyx to distances where the selectins or the ligands that are localized at the tips of the microvilli can form adhesive bonds with the EC counter-molecules to lead to rolling. These distances have been estimated to be at most 50 nm. Such penetrations, however, are only possible for a small population of very long microvilli that are several tenths of micrometers longer than their neighbors. A microvillus that is 0.7 μm in length would be able to penetrate this distance while undergoing free rolling only if its protrusion distance above its neighbors was nearly equal to the thickness of the glycocalyx, because the effective boundary for rolling at low shear is a displaced distance that is approximately equal to the average height of all the microvilli. The situation for tethered rolling differs dramatically. The contact time is at least two orders of magnitude longer than for free rolling and the contact force is also significantly greater. Thus, the penetration of the glycocalyx can be achieved by nearly all microvilli whether they are long or short, once an initial tether is established. Once rolling is initiated it is easily maintained because nearly all microvilli will have an impulse that is sufficient for the microvilli tips to approach the EC surface and form new adhesive bonds, provided that the selectins and/or their ligands are activated.

The two most important limitations of the present model are the treatment of the penetration of the glycocalyx for long microvilli and the uncertainty in the mechanical properties of the glycocalyx. The first limitation arises from the fact that the penetration force is based on contact forces for

rolling on a solid surface. The forces predicted provide an upper bound for the contact force because if any penetration occurs, this will reduce the magnitude of the pivot force in the free-rolling contact. A more sophisticated theory needs to be developed that takes account of the velocity and position of the microvillus tip. Further experiments are needed to confirm the mechanical penetration properties of the EC glycocalyx. The experiment in Lee et al. (1993) is the only existing experiment, to our knowledge, in which the mechanical properties of the surface glycocalyx have been measured. These experiments were performed on cultured fibroblasts, epithelial cells, and keratocytes, but not endothelial cells. Because the combined hydraulic and fiber-linked network resistance of the surface glycocalyx was similar for three cell types, one might conclude that, at least in the inner part of the glycocalyx, the pericellular matrix is a ubiquitous structure that is common to many cell types and that from a mechanical standpoint its properties may be similar for many cells. Additional experiments with larger particles (>30 nm) would be helpful in elucidating the penetration properties of the outer portion of the glycocalyx.

In conclusion, the theoretical framework developed herein has provided a quantitative basis for understanding a broad spectrum of problems in WBC rolling and tethering dynamics that have not been fully understood. The application of this model to WBC free rolling and initial tethering has revealed a highly nonlinear coupling between the hydrodynamic forces in the lubricating layer and the gravitational forces. This nonlinear coupling can magnify the tip contact forces nearly 100-fold above the resting state for the long microvilli that are involved in initial tethering. The model also predicts that only long microvilli can be involved in initial tethering near the shear threshold, but that once initiated, adhesive cell rolling is easy to maintain because the tethering resulted in marked increases in tip contact forces. The present theoretical model provides the first rational basis for quantitatively explaining the penetration of the endothelial glycocalyx in vivo. The model is able to explain why there is little rolling and adhesion on the arterial side of capillaries and why there is a shear threshold in postcapillary venules. Finally, the model provides a framework for analyzing the mechanical properties of the glycocalyx and suggests new experiments for elucidating its structure.

APPENDIX

For a sphere of radius R_c moving in a half space bounded by surface $z = 0$ (Fig. 1), define

$$\xi = \frac{R_c}{z}, \qquad (A1)$$

which ranges from 0 for a sphere infinitely far away from the surface to 1 for a sphere in contact with the surface. The hydrodynamic resistance functions in Eqs. 3–5 have well-known asymptotic expressions at $\xi = 0$

(Brenner, 1961; Goldman et al., 1967a, b), which are considered as "outer solutions." For the hydrodynamic resistance functions that are singular at $\xi = 1$, we use the method developed by Zhao et al. (1997) to first derive the forms of singularity, which are regarded as "inner solutions," and then obtain approximations valid over the whole range from $\xi = 0$ to 1 by matching the "outer" and "inner" solutions and fitting to the numerical solutions of Goldman et al. (1967a, b) or the series solution of Brenner (1961). The results are

$$\frac{h_1}{6\pi\mu R_c} = \frac{8}{15}\left[\ln(1 - \xi) + \xi\right]$$

$$- \left[1 + \frac{9}{16}\xi\right] + 0.072265\xi^{5.6328}, \quad (A2)$$

$$\frac{h_2}{6\pi\mu R_c^2} = -\frac{2}{15}\left[\ln(1 - \xi) + \xi + \frac{1}{2}\xi^2 + \frac{1}{3}\xi^3 + \frac{1}{4}\xi^4\right]$$

$$+ \frac{1}{8}\xi^4 - 0.10113\xi^{6.3295}, \qquad (A3)$$

$$h_3 = h_2, \qquad (A4)$$

$$\frac{h_4}{8\pi\mu R_c^3} = \frac{2}{5}\left[\ln(1 - \xi) + \xi + \frac{1}{2}\xi^2 + \frac{1}{3}\xi^3\right]$$

$$- \left[1 + \frac{5}{16}\xi^3\right] + 0.19989\xi^{5.9246}, \quad (A5)$$

$$\frac{h_5}{6\pi\mu R_c} = -\frac{1}{1 - \xi} + \frac{1}{8}\ln(1 - \xi), \qquad (A6)$$

$$\frac{h_6}{6\pi\mu R_c} = 1 + \frac{9}{16}\xi + 0.13868\xi^{1.4829}, \qquad (A7)$$

$$\frac{h_7}{4\pi\mu R_c^3} = 1 - \frac{3}{16}\xi^3 + 0.13187\xi^{3.7747}. \qquad (A8)$$

REFERENCES

Alon, R., S. Chen, K. D. Puri, E. B. Finger, and T. A. Springer. 1997. The kinetics of L-selectin tethers and the mechanics of selectin-mediated rolling. *J. Cell Biol.* 138:1169–1180.

Alon, R., D. A. Hammer, and T. A. Springer. 1995a. Lifetime of the P-selectin–carbohydrate bond and its response to tensile force in hydrodynamic flow [published erratum appears in *Nature.* 1995 Sep. 7;376: 86]. *Nature.* 374:539–542.

Alon, R., P. D. Kassner, M. W. Carr, E. B. Finger, M. E. Hemler, and T. A. Springer. 1995b. The integrin VLA-4 supports tethering and rolling in flow on VCAM-1. *J. Cell Biol.* 128:1243–1253.

Berlin, C., R. F. Bargatze, J. J. Campbell, U. H. von Andrian, M. C. Szabo, S. R. Hasslen, R. D. Nelson, E. L. Berg, S. L. Erlandsen, and E. C. Butcher. 1995. Alpha 4 integrins mediate lymphocyte attachment and rolling under physiologic flow. *Cell.* 80:413–422.

Brenner, H. 1961. The slow motion of a sphere through a viscous fluid towards a plane surface. *Chem. Eng. Sci.* 16:242–251.

Brinkman, H. C. 1947. A calculation of the viscous force exerted by a flowing fluid in a dense swarm of particles. *Appl. Sci. Res. A.* 1:27–34.

Bruehl, R. E., T. A. Springer, and D. F. Bainton. 1996. Quantitation of L-selectin distribution on human leukocyte microvilli by immunogold labeling and electron microscopy. *J. Histochem. Cytochem.* 44:835–844.

Chen, S., and T. A. Springer. 1999. An automatic braking system that stabilizes leukocyte rolling by an increase in selectin bond number with shear. *J. Cell Biol.* 144:185–200.

Chien, S., S. Usami, and R. Skalak. 1984. Blood flow in small tubes. *In* Handbook of Physiology: A Critical, Comprehensive Presentation of Physiological Knowledge and Concepts. S. R. Geiger, editor. American Physiological Society, Bethesda, MD. 217–249.

Feng, J., P. Ganatos, and S. Weinbaum. 1998. Motion of a sphere near planar confining boundaries in a Brinkman medium. *J. Fluid Mech.* 375:265–296.

Finger, E. B., K. D. Puri, R. Alon, M. B. Lawrence, U. H. von Andrian, and T. A. Springer. 1996. Adhesion through L-selectin requires a threshold hydrodynamic shear. *Nature.* 379:266–269.

Goldman, A. J., R. G. Cox, and H. Brenner. 1967a. Slow viscous motion of a sphere parallel to a plane wall. I. Motion through a quiescent fluid. *Chem. Eng. Sci.* 22:637–651.

Goldman, A. J., R. G. Cox, and H. Brenner. 1967b. Slow viscous motion of a sphere parallel to a plane wall. II. Couette flow. *Chem. Eng. Sci.* 22:653–660.

Hammer, D. A., and S. M. Apte. 1992. Simulation of cell rolling and adhesion on surfaces in shear flow: general results and analysis of selectin-mediated neutrophil adhesion. *Biophys. J.* 63:35–57.

Henry, C. B., and B. R. Duling. 1999. Permeation of the luminal capillary glycocalyx is determined by hyaluronan. *Am. J. Physiol. Heart Circ. Physiol.* 277:H508–H514.

Hu, X. P., and S. Weinbaum. 1999. A new view of Starling's hypothesis at the microstructural level. *Microvasc. Res.* 58:281–304.

Kaplanski, G., C. Farnarier, O. Tissot, A. Pierres, A. M. Benoliel, M. C. Alessi, S. Kaplanski, and P. Bongrand. 1993. Granulocyte-endothelium initial adhesion. Analysis of transient binding events mediated by E-selectin in a laminar shear flow [see comments]. *Biophys. J.* 64:1922–1933.

Lawrence, M. B., G. S. Kansas, E. J. Kunkel, and K. Ley. 1997. Threshold levels of fluid shear promote leukocyte adhesion through selectins (CD62L,P,E) [published erratum appears in *J. Cell Biol.* 1997 Apr. 7;137:261]. *J. Cell Biol.* 136:717–727.

Lawrence, M. B., and T. A. Springer. 1991. Leukocytes roll on a selectin at physiologic flow rates: distinction from and prerequisite for adhesion through integrins. *Cell.* 65:859–873.

Lee, G. M., F. Zhang, A. Ishihara, C. L. McNeil, and K. A. Jacobson. 1993. Unconfined lateral diffusion and an estimate of pericellular matrix viscosity revealed by measuring the mobility of gold-tagged lipids. *J. Cell Biol.* 120:25–35.

Ley, K. 1996. Molecular mechanisms of leukocyte recruitment in the inflammatory process. *Cardiovasc. Res.* 32:733–742.

Michel, E., S. Hillebrand, J. vonTwickel, B. Zernikow, and G. Jorch. 1997. Frequency dependence of cerebrovascular impedance in preterm neonates: a different view on critical closing pressure. *J. Cereb. Blood Flow Metab.* 17:1127–1131.

Puri, K. D., S. Chen, and T. A. Springer. 1998. Modifying the mechanical property and shear threshold of L-selectin adhesion independently of equilibrium properties. *Nature.* 392:930–933.

Schmid-Schönbein, G. 1987. Rheology of leukocytes. *In* Handbook of Bioengineering. R. Skalak and S. Chien, editors. McGraw-Hill, New York. 13.11–13.25.

Shao, J. Y., H. P. Ting-Beall, and R. M. Hochmuth. 1998. Static and dynamic lengths of neutrophil microvilli. *Proc. Natl. Acad. Sci. U.S.A.* 95:6797–6802.

Smith, M. J., E. L. Berg, and M. B. Lawrence. 1999. A direct comparison of selectin-mediated transient, adhesive events using high temporal resolution. *Biophys. J.* 77:3371–3383.

Stein, J. V., G. Cheng, B. M. Stockton, B. P. Fors, E. C. Butcher, and U. H. von Andrian. 1999. L-selectin-mediated leukocyte adhesion in vivo: microvillous distribution determines tethering efficiency, but not rolling velocity. *J. Exp. Med.* 189:37–50.

Tempelman, L. A., S. Park, and D. A. Hammer. 1994. Motion of model leukocytes near a wall in simple shear flow. *Biotechnol. Prog.* 10:97–108.

Tissot, O., A. Pierres, C. Foa, M. Delaage, and P. Bongrand. 1992. Motion of cells sedimenting on a solid surface in a laminar shear flow. *Biophys. J.* 61:204–215.

Tözeren, A., H. K. Kleinman, S. Wu, A. M. Mercurio, and S. W. Byers. 1994. Integrin alpha 6 beta 4 mediates dynamic interactions with laminin. *J. Cell Sci.* 107:3153–3163.

Tözeren, A., and K. Ley. 1992. How do selectins mediate leukocyte rolling in venules? *Biophys. J.* 63:700–709.

Tsay, R. Y., and S. Weinbaum. 1991. Viscous flow in a channel with periodic cross-bridging fibers: exact solutions and Brinkman approximation. *J. Fluid Mech.* 226:125–148.

Vink, H., and B. R. Duling. 1996. Identification of distinct luminal domains for macromolecules, erythrocytes, and leukocytes within mammalian capillaries. *Circ. Res.* 79:581–589.

von Andrian, U. H., S. R. Hasslen, R. D. Nelson, S. L. Erlandsen, and E. C. Butcher. 1995. A central role for microvillous receptor presentation in leukocyte adhesion under flow. *Cell.* 82:989–999.

Weinbaum, S. 1998. 1997 Whitaker distinguished lecture: models to solve mysteries in biomechanics at the cellular level; a new view of fiber matrix layers. *Ann. Biomed. Eng.* 26:627–643.

Zhao, Y., S. Chien, and R. Skalak. 1995. A stochastic model of leukocyte rolling. *Biophys. J.* 69:1309–1320.

Zhao, Y., R. Skalak, and S. Chien. 1997. Hydrodynamics in cell rolling and adhesion. *In* Advances in Bioengineering. B. Simon, editor. The American Society of Mechanical Engineers, New York. 79–80.